MAGNETIC RESONANCE IN CHEMISTRY
Magn. Reson. Chem. 2005; **43**: S140–S144
Published online in Wiley InterScience (www.interscience.wiley.com). DOI: 10.1002/mrc.1686

High-frequency EPR and ENDOR spectroscopy on semiconductor nanocrystals†

S. B. Orlinskii,[1] H. Blok,[1] E. J. J. Groenen,[1] J. Schmidt,[1]* P. G. Baranov,[2] C. de Mello Donegá[3] and A. Meijerink[3]

[1] Department of Molecular Physics, Huygens Laboratory, Leiden University, 2300 RA Leiden, The Netherlands
[2] A. F. Ioffe Physico-Technical Institute, RAS, 194021 St Petersburg, Russia
[3] Debye Institute, Utrecht University, Utrecht, The Netherlands

Received 28 April 2005; Revised 21 June 2005; Accepted 21 June 2005

EPR and ENDOR experiments at 95 GHz on ZnO nanoparticles reveal the presence of shallow donors related to interstitial Li and Na atoms. The experiments allowed, for the first time, to probe the effect of confinement on the shape of the electronic wave function. In addition, it is observed that the ^{67}Zn nuclear spins become polarized upon saturation of the EPR transition. This Overhauser effect is induced by the zero-point vibrations of the phonon system in the nanoparticles. Copyright © 2005 John Wiley & Sons, Ltd.

KEYWORDS: EPR; ENDOR; ZnO; nanocrystals

INTRODUCTION

In this contribution, we review the results of recent high-frequency EPR and ENDOR investigations on ZnO semiconductor nanocrystals. ZnO, with a direct band gap of 3.3–3.4 eV, attracts considerable attention because of its promising applications for UV light-emitting diodes and diode lasers. The attraction of ZnO nanocrystals is that the confinement of the electronic wave function allows the tuning of the optical and electronic properties. The effect of confinement on the electronic energy levels can easily be made visible by the change in the optical absorption spectra. We will show that high-frequency EPR and ENDOR spectroscopy is the method of choice to study the effect of confinement on the shape of the electronic wave function of shallow donors in ZnO nanocrystals. Interestingly, the saturation of the EPR transition of the shallow donors at high frequency and low temperature leads to an almost complete polarization of the ^{67}Zn ($I = 5/2$) nuclear spins in the nanoparticles. We argue that this Overhauser effect is caused by the zero-point fluctuations of the phonon system in the nanoparticles.

EXPERIMENTAL

The preparation of the samples of free-standing hydroxyl-capped ZnO nanocrystals in the form of dry powders was achieved using a modified version of methods reported in the literature.[1–3] Our method was based on the hydrolysis of Zn^{2+} ions in absolute alcohols (ethanol or 1-butanol), using either $LiOH \cdot H_2O$ for the Li-doped nanocrystals or NaOH for the Na-doped nanocrystals. The size of the nanocrystals was controlled by the growth duration. The average diameter of the nanocrystals was estimated by X-ray powder diffraction, based on the peak broadening due to the finite crystallite sizes (Scherrer's equation), and by UV–visible absorption spectroscopy, based on the size dependence of the band gap owing to quantum-size effects and by using a calibration curve.[1]

The EPR and ENDOR experiments were performed at 1.6 K using a pulsed 95 GHz EPR spectrometer.[4] The great advantage of working at this high microwave frequency is that a high spectral resolution is obtained in the EPR as well as in the ENDOR spectra. In addition, the use of pulsed microwave techniques considerably facilitates the observation of the ENDOR spectra.[4] The EPR spectra were recorded by monitoring the electron spin-echo (ESE) signal following a microwave $\pi/2$- and π-pulse sequence. The ENDOR spectra were obtained by monitoring the intensity of the stimulated echo, following three microwave $\pi/2$-pulses, as a function of the frequency of a radio-frequency pulse applied between the second and third microwave pulses.[5]

Probing the wave function of shallow donors in ZnO nanoparticles

In a recent paper, Park *et al.*,[6] on the basis of theoretical calculations, predicted that Li and Na behave as shallow donors if they occupy interstitial sites in ZnO. The reason to check the validity of this idea in nanometer-sized particles of ZnO is twofold. First, it is relatively easy to prepare this material and to dope it with Li and Na. Secondly, it allows us

†Presented as part of a special issue on High-field EPR in Biology, Chemistry and Physics.

*Correspondence to: J. Schmidt, Department of Molecular Physics, Huygens Laboratory, Leiden University, P. O. Box 9504, 2300 RA Leiden, The Netherlands. E-mail: mat@molphys.leidenuniv.nl

Contract/grant sponsor: Nederlandse Organisatie voor Wetenschappelijk Onderzoek (N.W.O.).
Contract/grant sponsor: SENTINEL Network.

not only to identify the shallow donor via the ENDOR signals of the nuclear spin of the binding core and the nuclear spins of the surrounding ^{67}Zn ions but also to probe the effects of confinement on its spatially extended wave function by varying the particle size in the quantum-size regime.[7]

Figure 1 shows the ESE-detected EPR spectrum of a dry powder sample of Li-doped ZnO nanoparticles with an average diameter of 3.4 nm after ultraviolet irradiation at 1.6 K. The signal labeled I at 3.448 T with a linewidth of 6.0 mT is assigned to the interstitial Li donor. Its average g-value $g_{av} = 1.9666$ differs somewhat from the $g_{||} = 1.9569$ and $g_{\perp} = 1.9552$ values obtained for the interstitial hydrogen donor in a single crystal of ZnO.[8] The linewidth however corresponds very well with $g_{||} - g_{\perp} = 0.0017$ obtained for the interstitial hydrogen donor and taking into account the random character of the powder sample. The EPR signal labeled II around 3.3875 T is assigned to a Na-related center whereas the signal labeled III is identified either as originating from the deep Li_{Zn} acceptor[9] or from the Zn vacancy.[10] Here, we will concentrate on the EPR signal I assigned to the shallow Li donor.

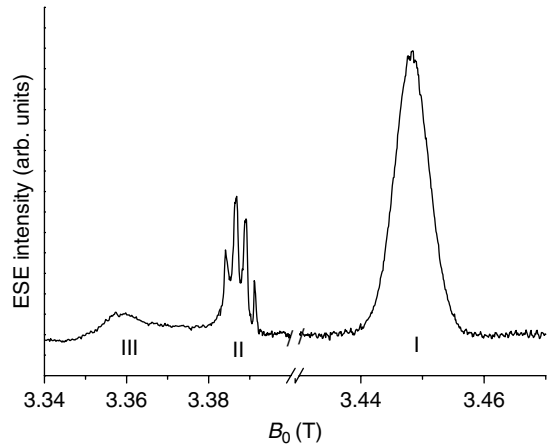

Figure 1. The ESE-detected EPR spectrum at 94.9 GHz of a dry powder sample of Li-doped ZnO nanoparticles with an average diameter of 3.4 nm after UV-irradiation. The assignment of the transitions labelled I to III is indicated in the text.

The EPR signal I in Fig. 1 is assigned to a donor because g_{av} is smaller than the g-value of a free electron. The shallow character becomes clear from the dependence of g_{av} on the size of the nanoparticles. We find that $g_{av} = 1.9628$ for particles with a diameter of 4.4 nm increases to $g_{av} = 1.9670$ for particles with a diameter of 3.2 nm. This shift towards the free-electron g_e-value has been observed by Zhou *et al*.[11] and is caused by the confinement of the hydrogen-like 1s-type wave function of shallow donors when the Bohr radius becomes comparable to the size of the nanoparticles. The effect is explained by the reduction of the admixture of valence-band states and higher-lying conduction bands by the increase of the band-gap energy and the energy of higher-lying conduction bands upon the reduction of the size of the nanoparticles.[12]

In Fig. 2, the ENDOR signals as obtained on the EPR signal I of the shallow donor are presented. To understand these results, we consider the isotropic hyperfine interaction or Fermi contact term a_i that reflects the spin density of the donor electron wave function (Ψ) at the site of the nucleus (r_i).

$$a_i = (8\pi/3) g_e \beta_e g_{ni} \beta_n |\Psi(r_i)|^2 \quad (1)$$

where g_e is the electronic g-factor, β_e is the electronic Bohr magneton, g_{ni} is the g-factor of nucleus i, and β_n is the nuclear magneton. The related ENDOR transition frequencies are

$$\nu_{ENDORi} = h^{-1} |g_{ni} \beta_n B_0 \pm a_i/2| \quad (2)$$

Expression (2) predicts that each nucleus i gives rise to two ENDOR transitions symmetrically placed around its nuclear Zeeman frequency $g_{ni}\beta_n B_0/h$ when the quadrupole interaction is neglected and when $a_i < g_{ni}\beta_n B_0$.

First, in Fig. 2, symmetrically around the Zeeman frequency of ^{67}Zn ($I = 5/2$, abundance 4.1%) at 9.2 MHz, a broad, unresolved set of ENDOR lines of ^{67}Zn spins is observed. From the multitude of lines seen for a bulk crystal[8] it is clear that we are indeed dealing with a delocalized electron of a shallow donor that interacts with a

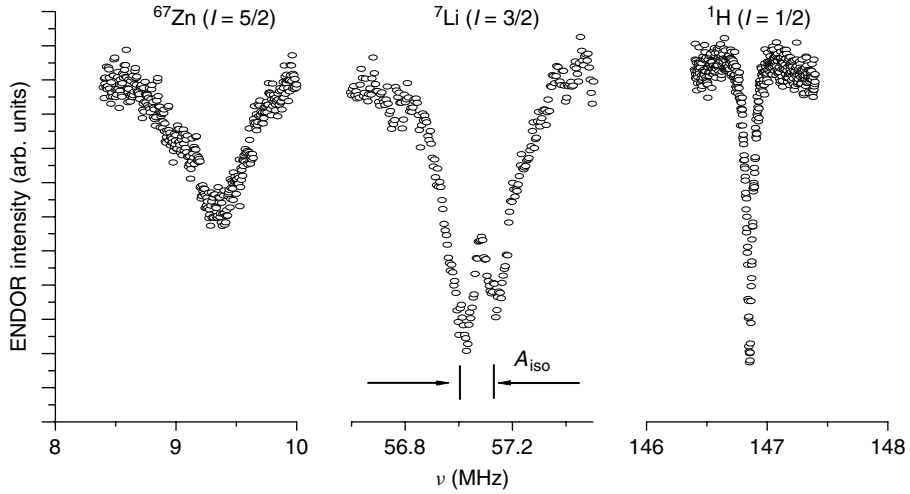

Figure 2. The ENDOR transitions of the ^{67}Zn, ^{7}Li, and ^{1}H nuclear spins observed in the EPR signal I (Fig. 1) of the shallow Li-related donor.

large number (tens) of ^{67}Zn nuclei. Secondly, symmetrically around the Zeeman frequency of ^{7}Li ($I = 3/2$, abundance 92.5%) at 57.1 MHz, two ENDOR lines are present, separated by 90 kHz, that are assigned to ^{7}Li. These signals are taken as proof that Li^+ forms an interstitial core for the shallow donor electron in the ZnO nanoparticle.

In Fig. 2, an ENDOR line with a width $\Delta\nu$ = 60 kHz exactly at the Zeeman frequency of ^{1}H is also seen. From the width we deduce a ^{1}H h.f. interaction smaller than 60 kHz. This should be compared with our previous observation on the hydrogen-related shallow donor in a bulk crystal of ZnO where two ENDOR lines were found with a hyperfine splitting of 1.4 MHz.[8] We conclude that the observed ENDOR lines originate in the hydrogen atoms present in the $Zn(OH)_2$ capping layer where the density of the electronic wave function is very small.

To check whether interstitial Na can also act as a shallow donor in ZnO, we have performed similar EPR and ENDOR experiments on ZnO nanoparticles that were treated with NaOH. In such ZnO nanoparticles with a diameter of 3.0 nm and after UV-illumination, we observe again three EPR signals analogous to the Li-doped sample. The EPR signal similar to I in Fig. 1 with a $g_{av} = 1.9592$ is assigned to a shallow Na-related donor. In Fig. 3, the result of an ENDOR experiment on this signal is presented that reveals two transitions with a splitting of 300 kHz symmetrically placed around the Zeeman frequency of ^{23}Na at 38.97 MHz. We consider this as proof of the presence of a shallow donor related to interstitial Na in the ZnO lattice.

The observation of the ^{7}Li ENDOR signals allows us to measure the effect of confinement on the wave function of the shallow Li donor directly. To this end, we have measured the dependence of the splitting of the two ^{7}Li hyperfine components as a function of the radius R of the ZnO core of the nanoparticles, and the results are presented in Fig. 4. The splitting of the two ^{7}Li ENDOR lines is equal to the isotropic hyperfine interaction of the unpaired electron spin with the ^{7}Li nuclear spin and thus proportional to the density of the electronic wave function at the position of the Li^+ core. This Li^+ core is considered to be at (or near) the center of the ZnO nanoparticle, on the basis of the small size of the hydrogen hyperfine interaction. In the same figure, an AR^{-3}+ B curve is plotted (solid line). Down to $R = 1.6$ nm, the experimental results follow this dependence quite closely while for smaller radii there is a deviation to smaller values.

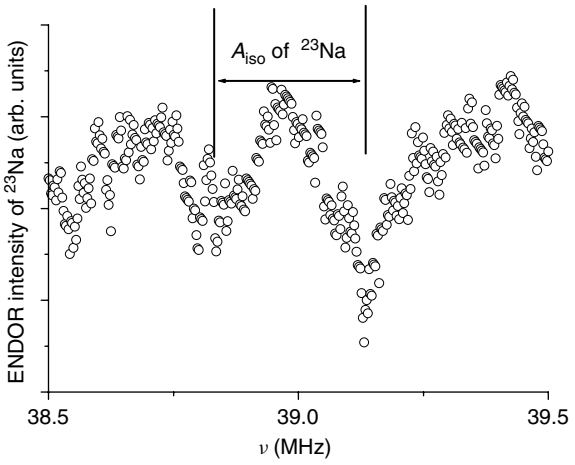

Figure 3. The ENDOR transitions of ^{23}Na as observed in the EPR signal of the shallow donor in Na-doped ZnO nanoparticles with an average size of 3.0 nm. The two ENDOR transitions are symmetrically placed around the Zeeman frequency of ^{23}Na at 38.97 MHz with a splitting of 300 kHz.

In Fig. 5, in a plot similar to that in Fig. 4, the width of the ENDOR line of the ^{1}H nuclei in the $Zn(OH)_2$ capping layer is shown as a function of R. This width is taken as a measure of the distribution of the hyperfine fields in the capping layer. For particles with R between 2.2 and 1.5 nm, the R^{-3} dependence describes the experimental data, but for smaller radii, the width of the ENDOR line no longer seems to increase.

To test whether the observed size dependence of the density of the wave function at the ^{7}Li nucleus in the ZnO core and its distribution in the $Zn(OH)_2$ capping layer can be explained with the Effective Mass Approximation, we have introduced a trial wave function with appropriate boundary conditions to simulate the envelope function of the shallow donor electron. By using a variational procedure in which the total energy is calculated numerically and minimized, the density of the wave function at the center of the ZnO core, where the Li nucleus is supposed to be located, and at the interface of the ZnO core and the $Zn(OH)_2$ capping layer is derived.[13]

In Fig. 4, the variation of the density of the electronic wave function at the position of the ^{7}Li nucleus, as calculated with the method described above, is indicated by the dotted line. For values of R smaller than 1.5 nm, no stable solution

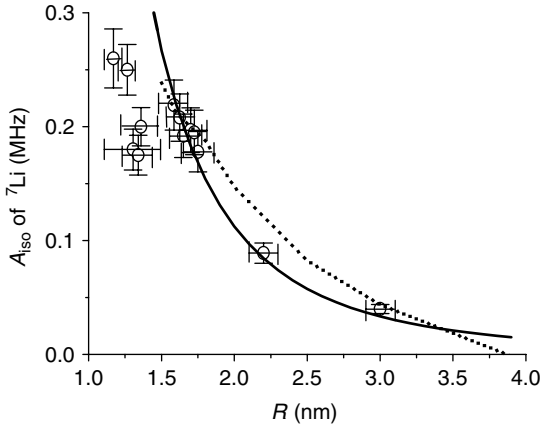

Figure 4. The isotropic hyperfine interaction A_{iso} of the ^{7}Li nuclear spin of the shallow Li donor in nanoparticles of ZnO with radii between 3.0 and 1.1 nm. The black dots indicate the hyperfine splitting as observed in the ENDOR spectra at $T = 1.6$ K. The error bar in the values of A_{iso} is estimated from the noise in the ENDOR spectra. The variation in the size of the particles is derived from TEM and XRD measurements. The solid line is a least-square fit to the measured values of A_{iso} for the particles with radii between 3.0 and 1.5 nm using the function $AR^{-3} + B$ with $A = 745.4$ kHz $(nm)^3$ and $B = 10$ kHz. The dotted line represents the electron density at the position of the Li core as calculated with the model described in the text.

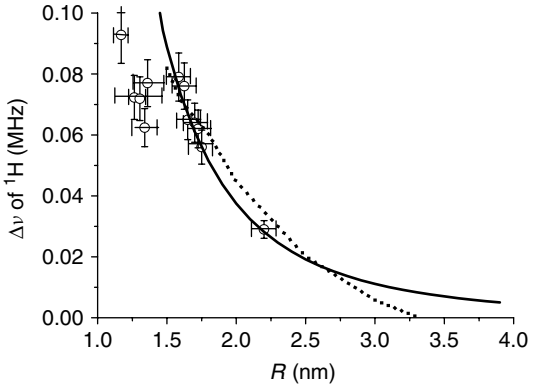

Figure 5. The width of the ENDOR line of the ^{1}H nuclear spins in the $Zn(OH)_2$ capping layer of ZnO nanoparticles with various radii. The black dots indicate the linewidth as observed in the ENDOR spectra at $T = 1.6$ K. The error bars are obtained in a similar fashion as in Fig. 4. The solid line is a least-square fit to the measured values of the linewidth for the particles with radii ranging from 2.2 to 1.5 nm using the function $AR^{-3} + B$ with $A = 276.8$ kHz $(nm)^3$ and $B = 3$ kHz. The dotted line represents the electron density at the $ZnO/Zn(OH)_2$ interface as calculated with the model described in the text.

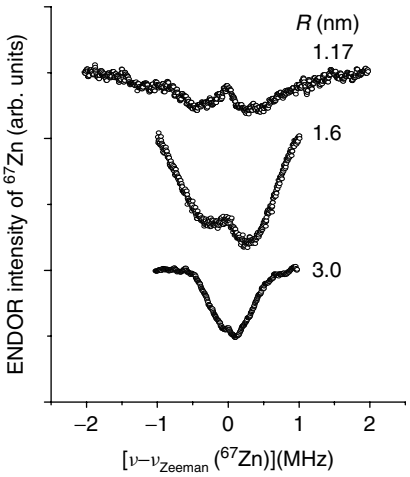

Figure 6. The ENDOR spectra of the ^{67}Zn ($I = 5/2$) nuclear spins in the ZnO nanoparticles with radii of 1.17, 1.6, and 3.0 nm. Each spectrum consists of many unresolved lines placed symmetrically around the Zeeman frequency of the ^{67}Zn nuclear spins at 9.2 MHz.

was found. Similarly, in Fig. 5, the variation of the calculated density of the wave function at the interface of the ZnO core and the $Zn(OH)_2$ capping layer is indicated by the dotted line. This calculated value was assumed to be proportional to the distribution of hyperfine fields experienced by the ^{1}H nuclei in the $Zn(OH)_2$ layer, and thus to the linewidth of the ^{1}H ENDOR line.

Our simple analytical model based on the Effective Mass Approximation does not give a stable solution for the electronic wave function of shallow donors in the quantum confinement regime, i.e. in semiconductor nanocrystals with radii of the order of or smaller than the Bohr radius in the bulk material. We give two reasons for this failure. First, the use of the bulk value for the effective mass of the electron is not permitted. This parameter reflects the effect of the periodic potential of a (infinite) semiconductor crystal and this approximation breaks down for the nanometer-sized nanocrystal. In other words, the allowed values for the wave vector **k** become discrete and the energy eigenvalues are those for an electron of mass m_0 in a box. Secondly, the definition of a dielectric constant, as a consequence of the Lorentz relation, does not apply to a nanocrystal. As demonstrated by Ödğüt *et al.*,[14] the effective screening function in a confined system depends on the size of and on the position in the nanoparticle. We believe that an appropriate description of the electronic wave function should be found by using molecular-cluster-type calculations as carried out recently by Melnikov and Chelikowsky[15] for the electronic wave function of shallow P donors in Si nanoparticles.

In addition to the hyperfine interactions with the ^{7}Li and ^{1}H nuclei, information is also supplied by the hyperfine interactions with the ^{67}Zn nuclei. In Fig. 6, the ENDOR spectra of the ^{67}Zn nuclei are presented (symmetrically placed around the ^{67}Zn Zeeman frequency at about 9.2 MHz) for ZnO particles of various radii. The remarkable observations are that the ENDOR band broadens upon size reduction and develops a dip around the Zeeman frequency of the ^{67}Zn nuclear spins. The dip becomes more prominent and broader when the radius of the ZnO core is reduced from $R = 3.0$ via 1.6 to 1.17 nm. The broadening of the ENDOR band tells us that the maximum density of the electronic wave function increases with reduction in the size of the nanoparticles. The disappearance of the ENDOR signals close to the ^{67}Zn Zeeman frequency, which corresponds to a virtual zero density of the electronic wavefunction, shows that the density of the envelope wave function at the interface also increases as a result of the confinement. In other words, the dip in the ENDOR spectrum indicates that for the small particles, even at the interface, the Zn nuclei carry nonzero spin density. This conclusion is in line with our observation that the electron density at the $ZnO/Zn(OH)_2$ interface, as measured from the linewidth of the ^{1}H ENDOR signal, increases with decreasing size of the particles. It is interesting to note that estimates of the electron density at the $ZnO/Zn(OH)_2$ interface, using either the width of the dip in the ^{67}Zn ENDOR signal or the linewidth of the ^{1}H ENDOR signal and using the amplification factors for Zn and H,[8] yield about the same value. Our conclusion that the electron density at the surface increases with decreasing size of the nanoparticle is at variance with the results of the calculations of Melnikov and Chelikowsky[15] for the P-doped Si nanoparticles. These calculations indicate that, upon reduction of the size of the nanoparticles, the electron density concentrates in the P–Si nearest-neighbour bond and becomes very small at the surface.

In summary, our results show that we can monitor the change of the electronic wave function of a shallow donor in a ZnO semiconductor nanoparticle when entering the regime of quantum confinement by using the nuclear spins in the semiconductor nanocrystals as probes. Our model, based on the Effective Mass Approximation, does not yield

an appropriate description of the electronic wave function when the radius of the nanoparticle is reduced below the Bohr radius. We suggest that molecular, cluster-type calculations should be carried out to describe the observed behaviour.

Dynamic nuclear polarization of ^{67}Zn nuclear spins in ZnO nanoparticles

In Fig. 7, we present hole burning in the EPR line detected at 95 GHz and 1.6 K of the shallow Li donor in ZnO nanoparticles with a diameter of 3.4 nm. The hole arises after preirradiation with microwaves during 2 min at one position in the EPR line. The EPR line is inhomogeneously broadened as a result of the anisotropy of the **g**-tensor and the random character of the orientation of the nanoparticles. The hole is thought to be caused by dynamic nuclear polarization of the ^{67}Zn nuclear spins through the Overhauser effect induced by the zero-point fluctuations of the phonon system. The mechanism is analogous to the dynamic nuclear polarization effects observed in bulk ZnO crystals doped with shallow H-donors.[16] The interesting aspect is that phonon modes with the required frequency of 95 GHz needed to induce the cross relaxation typical for the Overhauser effect do not fit into the nanocrystals! This observation may indicate that the phonons are not concentrated in one nanoparticle but extend over clusters of ZnO particles.

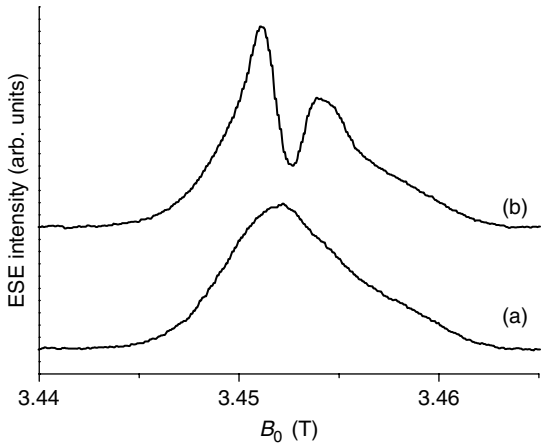

Figure 7. (a) the EPR line of the shallow Li donor in a dry powder of ZnO nanoparticles with a diameter of 3.4 nm observed at a frequency of 94.9 GHz and a temperature of 1.5 K. (b) The same EPR line recorded after preirradiation with microwaves during 2 min at one position in the EPR line. It is seen that a hole is burnt and an antihole develops. These effects are attributed to dynamic nuclear polarization of the ^{67}Zn nuclear spins in the nanocrystals.

Acknowledgements

This work forms part of the research program of the Netherlands Foundation for Fundamental Research of Matter (F.O.M.) and the Technology Foundation STW, both with financial support from the Nederlandse Organisatie voor Wetenschappelijk Onderzoek (N.W.O.). Financial support from the SENTINEL Network in the framework of the 5th EC Science program is acknowledged. P.G.B. acknowledges support by RFBR and the Project of RAS 'Spin-dependent effects in solids and spintronics.'

REFERENCES

1. Meulenkamp EA. *J. Phys. Chem. B* 1998; **102**: 5566.
2. Hu Z, Oskam G, Searson PC. *J. Coll. Interf. Sci.* 2003; **263**: 454.
3. Noack V, Eychmuller A. *Chem. Mater.* 2002; **14**: 1411.
4. Disselhorst JAJM, van der Meer HJ, Poluektov OG, Schmidt J. *J. Magn. Reson. A* 1995; **115**: 183.
5. Mims WB. *Electron Paramagnetic Resonance*. Geschwind S (ed.). Plenum: New York, 1972.
6. Park CH, Zhang SB, Wei S-H. *Phys. Rev. B* 2002; **66**: 073 202.
7. Orlinskii SB, Schmidt J, Baranov PG, Hofmann DM, de Mello Donegá C, Meijerink A. *Phys. Rev. Lett.* 2004; **92**: 047 603.
8. Hofmann DM, Hofstaetter A, Leiter F, Zhou H, Henecker F, Meyer BK, Orlinskii SB, Schmidt J, Baranov PG. *Phys. Rev. Lett.* 2002; **88**: 045 504.
9. (a) Schirmer OF. *J. Phys. Chem. Solids* 1968; **29**: 1407; (b) Schirmer OF, Zwingel D. *Solid State Commun.* 1970; **8**: 1559.
10. Taylor AL, Filipovich G, Lindeberg GK. *Solid State Commun.* 1970; **8**: 1359.
11. Zhou H, Hofstaetter A, Hofmann DM, Meyer BK. *Microelectron. Eng.* 2003; **66**: 59.
12. Rodina AV, Efros AL, Rosen M, Meyer BK. *Mater. Sci. Eng. C* 2002; **19**(1–2): 435.
13. Orlinskii SB, Schmidt J, Groenen EJJ, Baranov PG, de Mello Donegá C, Meijerink A. *Phys. Rev. Lett.* 2005; **94**: 097 602.
14. Öğüt S, Burdick R, Saad Y, Chelikowsky JR. *Phys. Rev. Lett.* 2003; **90**: 127 401.
15. Melnikov DV, Chelikowsky JR. *Phys. Rev. Lett.* 2004; **92**: 046 802.
16. Blok H, Orlinskii SB, Schmidt J, Baranov PG. *Phys. Rev. Lett.* 2004; **92**: 047 602.